# MF2007 - Workshop A

Adam Lang 861110-3956
Gabriel Andersson Santiago 910706-4538
Andreas Fröderberg 880730-7577

April 7, 2016

## Parameter identification

This section covers the methods behind finding the parameters to enter into the model to get the biggest similarity to the physical plant

### Level 1

To identify the parameters of the DC motor, firstly an idealized model is studied theoretically to understand which physical parameters that affect the performance of the motor. In the Laplace frequency domain, a model of the motor without inductance can be expressed as

$$X = \frac{k(1+\frac{1}{Rd})}{s\frac{J_t}{\frac{k^2}{R}+d}+1}U, \tag{1}$$

where $X$ is the rotational speed, $U$ is the input voltage, $k$, $R$ and $d$ are the electric motor constant, internal resistance and the viscous friction. The variable $J_t$ represents the total inertia of the motor and the load. With the load inertia after a gear with gear ratio $n$, the total inertia is

$$J_t = J + \frac{J_{load}}{n^2}. \tag{2}$$

Here, the load inertia and the inertia of the motor are separated and the motor inertia from the datasheet is presumed to be correct, leaving only the load inertia as an unknown. Now the relations between the motor parameters and the time performance can be seen. The time constant is given by the term

$$\frac{J_t}{\frac{k^2}{R}+d} \tag{3}$$

and as such contains all the parameters of the motor. According to the final value theorem, the steady state value from a step input is given by setting $s = 0$ and therefore the steady state gain is given by

$$k(1+\frac{1}{Rd}). \tag{4}$$

This contains only one unknown parameter. Therefore, to estimate the viscous friction parameter $d$, it is suitable to examine and match the steady state rotational speed of the real system and the model. Since this model contains no static friction which is probably present in the real system, the test is conducted at maximum permissable input voltage to minimize the disturbances in the test data. Since the desired value does not depend on frequency, only a square wave input is used to simulate steps in both directions.

Now that the friction parameter is presumed to be correct and fixed, the time constant in Equation (3) only has one unknown, the load inertia. This is estimated from taking the time constant from step inputs, simulated by a square wave signal. Again, to minimize model disturbances caused by the static

friction present in the real system, the square wave is run at a full 24 V.
The tuning can be seen in Figure 1. After the viscous friction is modeled, values on the inertia of the system is adjusted to fit the real motor. The end result after the parameters have been tuned can be seen in Figure 1.

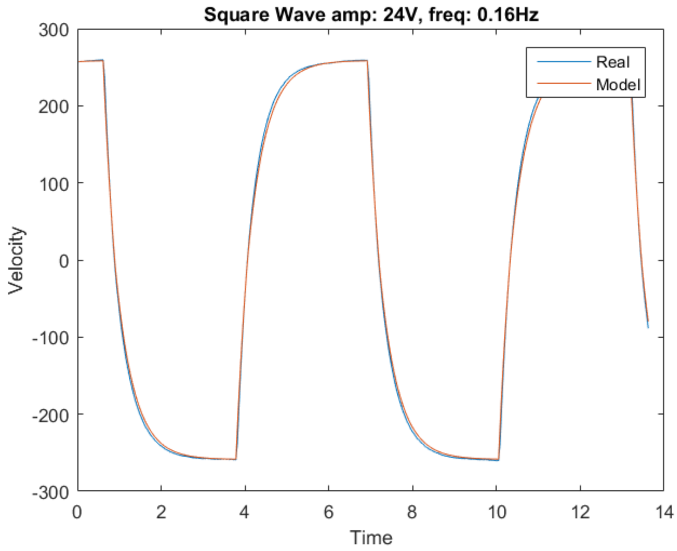


Figure 1: Velocity output from the motor and the model when tuned for both viscous friction and inertia.

After tuning, the inertia of the load is found to be $6 \cdot 10^{-5}$ kgm2 and the viscous friction is $1.35 \cdot 10^{-1}$ Nms/rad. The problem with this linear friction model is that even though it can be made to fit a certain velocity level set point, because of the nonlinearity in the real system the model performance will differ when it is run further away from the set point. In Figure 2, the system is run with the same parameters but at a lower voltage, yielding big discrepancies between the model and the system.

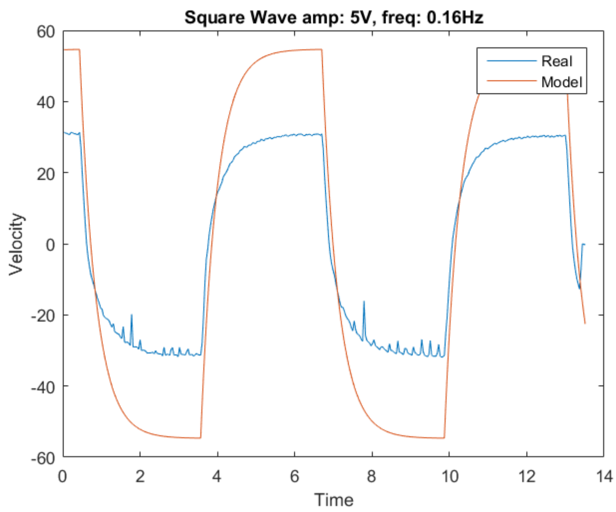


Figure 2: Model performance when not at set point.

## Level 2

As could be seen in the earlier friction model, it did not incorporate the effects of static friction which led to inaccuracy in the model when varying the rotational speed. A model which captures the real behaviour of the system is used here, called the Karnop friction model. In addition to the linear friction, the static friction is taken into account by adding a stick-slip zone where the friction tourque is equal to the applied torque. The model is given by the equation

$$M_f = d\dot{\phi} + F_c sgn(\dot{\phi}), \tag{5}$$

with the friction torque $M_f$ and the static friction $F_c$. This friction is the maximum static friction torque that can be applied in the stick slip zone. There is now one more design parameter that needs to be tuned, $F_c$. The linear friction is still most prominent when at high velocities and the static friction is the strongest when at low velocities. The inertia is decided solely from the rise time and should not differ much from the previous model. Firstly, the step response to a 5 V square wave is examined to determine the static friction. When the static friction is set, the response to a square wave at 24 V is examined and $d$ is adjusted to fit the viscous friction. A sine of low amplitude is then run to test the behaviour around the stick slip area, i.e. at low speeds.

The stick slip zone span is set to be 1 rad/s. The new viscous friction is then $1 \cdot 10^{-5}$ Nms/rad and the static friction is $1.5 \cdot 10^{-3}$ Nm. In Figure 3 the tuned model is run at the full voltage range of the motor. The model follows the real plant very well.

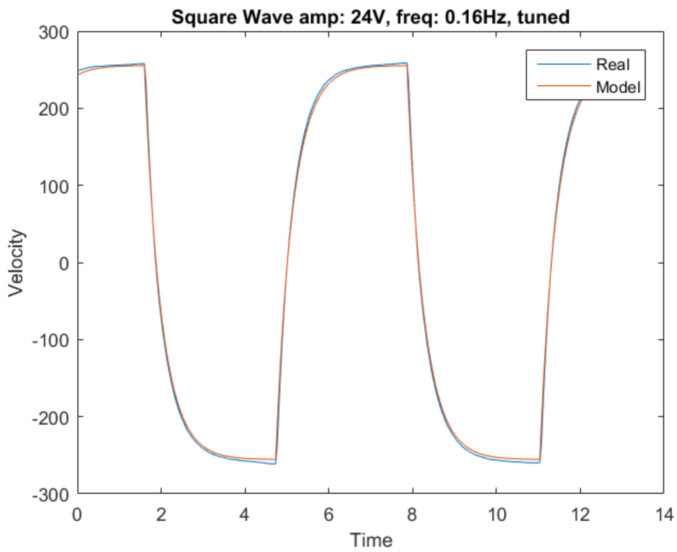


Figure 3: Velocity response of motor and model at 24V amplitude when tuned for both static and dynamic friction.

To verify that the model works also at voltages outside the set point, the model is run at a 5 V amplitude. The result is displayed in Figure 4.

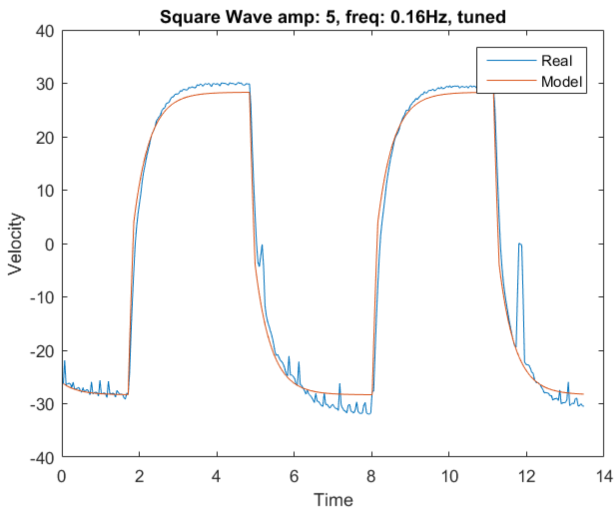


Figure 4: Model compared to system when at low voltages.

The model performance is substantially improved from the linear model, even outside the set points. The model perfomance during sine input is displayed in Figure 5.

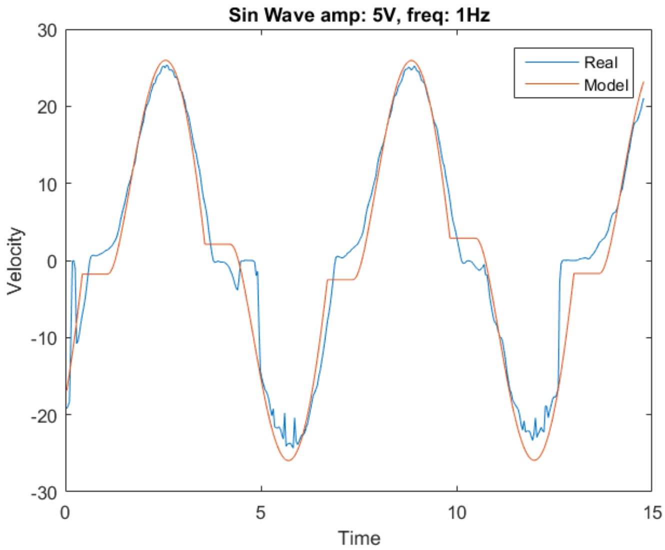


Figure 5: Velocity response of a sine wave at 5V amplitude of the motor and tuned model

The inflexion points when the voltage is too low to overcome the static friction is captured by the model.

# Velocity control

The parameters generated in the previous section are used to design the controller for the motor. For the design, a simplified model without motor inductance is used in MATLAB to place the poles and estimate the behaviour of the system. Furthermore, a non-linear model with Karnop friction is used in SIMULINK to simulate the behaviour of the system with the controller implemented. Finally, the design is run on the actual motor for verification of plant model and controller.

## Level 1

Controlling the velocity is done with a PI controller. To best control the performance, the controller is designed in discrete time.

The rule of thumb for sample time of a system states that the system should be sampled at 4-10 times the rise time of the plant in open loop. Using the simplified model in MATLAB and the commando `stepinfo`, the rise time is extracted and the sampling time is set to 10 times the rise time.

To get the desired performance of the closed loop system, the poles are placed directly in the discrete plane. First, the plant is converted from continuous to discrete space by Zero Order Hold (ZOH), with the sampling time derived earlier.The new sytem matrices are given by the equations

$$\Phi = e^{AT_s} \tag{6}$$

and

$$\Gamma = \int_0^{T_s} e^{A(t-s)} B \mathrm{d}s. \tag{7}$$

Output feedback is used to create the closed loop system. The model of the plant is given in (1) and is here rewritten as

$$\frac{B}{A} = \frac{a}{s+b} \tag{8}$$

,to simplify the equations. Firstly, the feedback polynomial $\frac{S}{R}$ is derived. This is given by

$$\frac{S}{R} = \frac{s_1 z + s_0}{z-1}. \tag{9}$$

The system is then closed, yielding the pole polynomial

$$AR + BS = z^2 + (as_1 + b - 1)z + as_0 - b. \tag{10}$$

The system is of order one so one closed loop pole given by

$$A_m = z - p_1 \tag{11}$$

is placed with an additional pole given by the observer polynomial

$$A_o = z - p_2 \tag{12}$$

This yields the Diophantine equation

$$A_m A_o = AR + BS. \tag{13}$$

Solving for (13) the unknown controller parameters $s_0$ and $s_1$ are found to be

$$s_0 = \frac{p1p2 + b}{a} \tag{14}$$

and

$$s_1 = -\frac{b + p_1 + p_2 - 1}{a}. \tag{15}$$

The $T$ polynomial is given by

$$T = t_0 A_o \tag{16}$$

where $t_0$ is a static value so that the steady state gain of the closed loop system is 1. Using the final-value theorem for discrete systems, one yields

$$t0 = \left(\frac{B}{A_m}\right)^{-1} \tag{17}$$

evaluated in $z = 1$. The control law is then found as,

$$R(z)u(z) = T(z)r(z) - S(z)y(z) \tag{18}$$

and in numerical form,

$$(z - 1)U(z) = t_0(0.420z - 0.376)r(z) - (0.533z - 0.489)y(z) \tag{19}$$

In Figure 6a is the response from a square wave with 50 rad/s and 0.5Hz shown. In Figure 6b the voltage response for the same input is plotted.

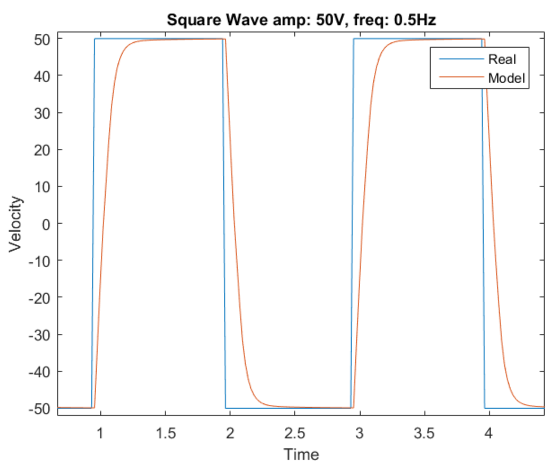


(a) Velocity response

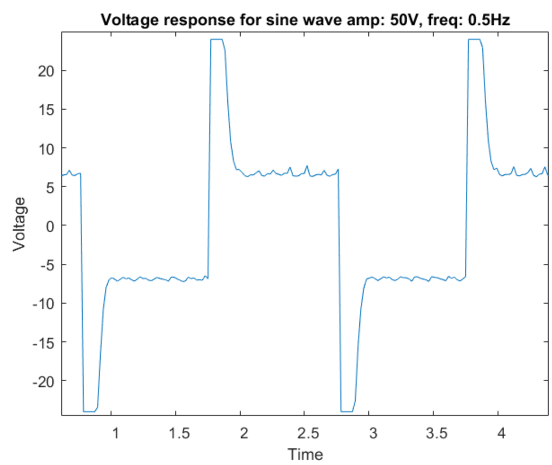


(b) Voltage response

Figure 6: Response for square wave 50 rad/s and 0.5Hz

It can also be seen in Figure 7 the plot that the steady state error is less than the specified 0.5 rad/s. And that there is no overshoot.

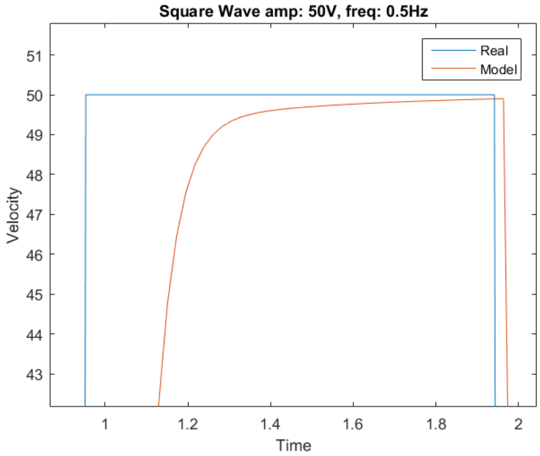


Figure 7: Zoomed plot of the Velocity response

In Figure 8a is the response from input of $\varphi_{ref} = 10sin(2\phi 0.2t)$ shown.

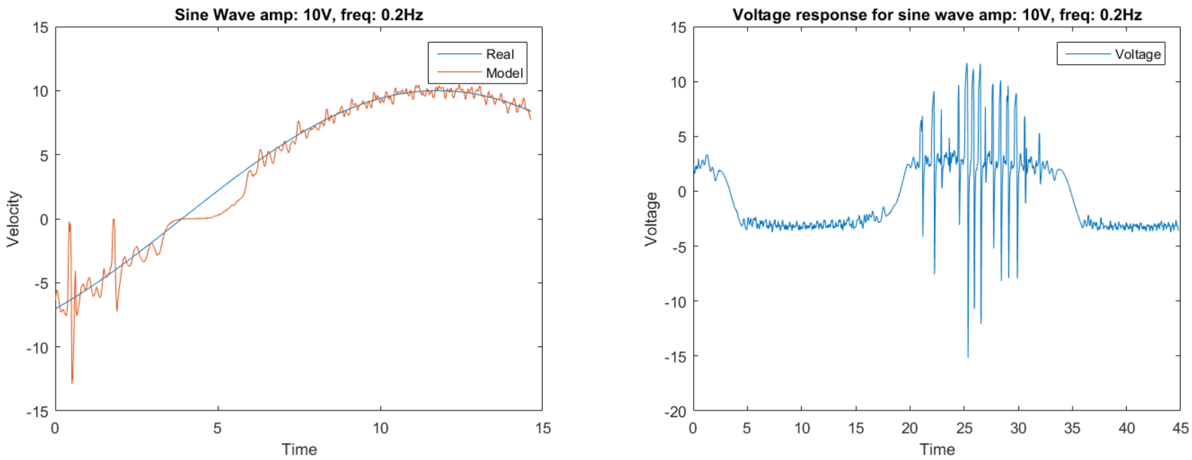


(a) Velocity response

(b) Voltage response

Figure 8: Response for sine wave 10 rad/s and 0.2Hz

In Figure 9a is the response from the reference input of $\varphi_{ref} = 10sin(2\pi 0.2t)$ shown. In this plot is the rotor loaded with a torque by holding it.

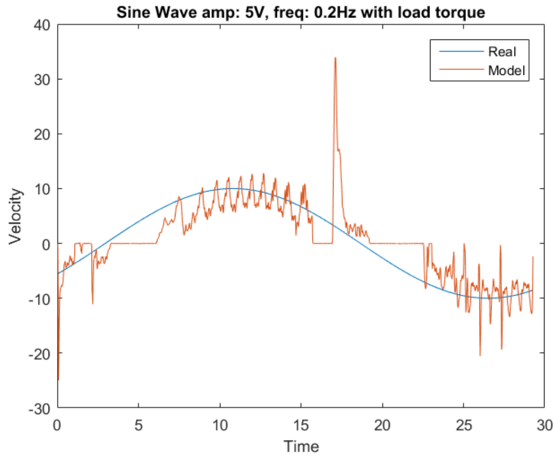


(a) Velocity response

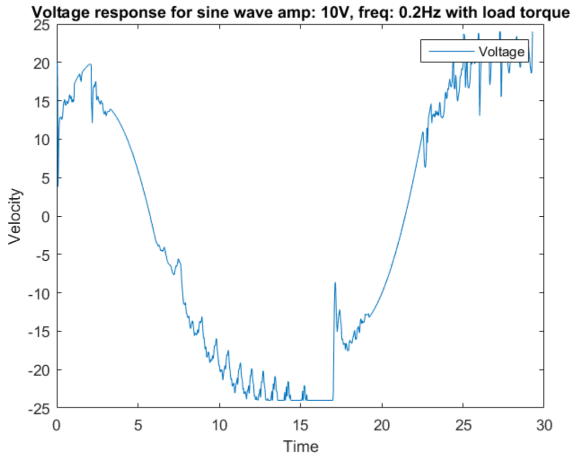


(b) Voltage response

Figure 9: Response for sine wave 10 rad/s and 0.2Hz

The controller follows the sine input well when undisturbed. When disturbing the motor with an extra load, it sources much more voltage and does not always have the power to negate the disturbances.

# Position Control

The open loop system for the is reached by integrating the velocity system. Therefore, the system contains a pure integrator pole. The new system is written as

$$G(s) = \frac{a_c}{s^2 + b_c s} \tag{20}$$

in the continuous case. To find a suitable sampling rate, the bandwidth of the open loop controller is examined using a Bode plot and the sampling rate is chosen to be 10-30 times faster. With a bandwidth of 5.78, the sampling rate is chosen as 10 times this. The final sampling time is then 0.11 s. Finally, before the control design is done, the system is sampled with ZOH, yielding the system

$$G_0(z) = \frac{az + b}{z^2 + cz + d}, \tag{21}$$

where the numerical values are discplayed in the table below.

Table 1: Numerical values of discretized closed loop system.

| | |
|---|---|
| a | 0.421 |
| b | 0.389 |
| c | -0.20 |
| d | 0.01 |

## Level 1

For this control, a discrete PID controller is used with transfer function

$$\frac{S}{R} = \frac{s_2 z^2 + s_1 z + s_0}{(z-1)(z+r_0)}. \tag{22}$$

The control design process is similar to the one used with the velocity controller with the addition of a higher order system. The resulting control law becomes

$$\big((z-1)(z+0.784)\big)u(z) = (13.1z^2 - 14.9z + 4.87)r(z) - (3.06z^2)y(z) \tag{23}$$

where the observer polynomial and the closed loop polynomial is,

$$A_m = (z - 0.1)(z - 0.1)$$
$$A_o = z^2.$$

In Figure 10a the response from the controller can be seen and in Figure 10b the voltage response is plotted.

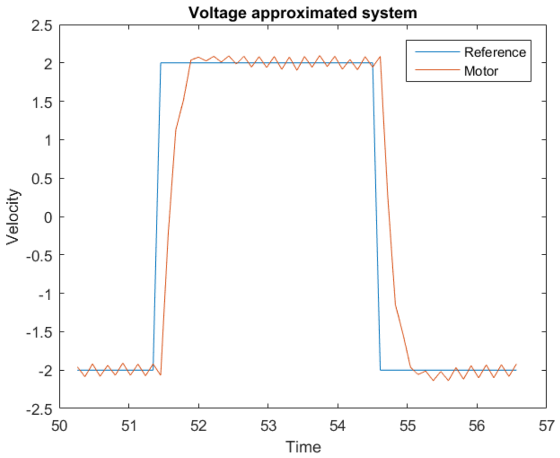


(a) Position response

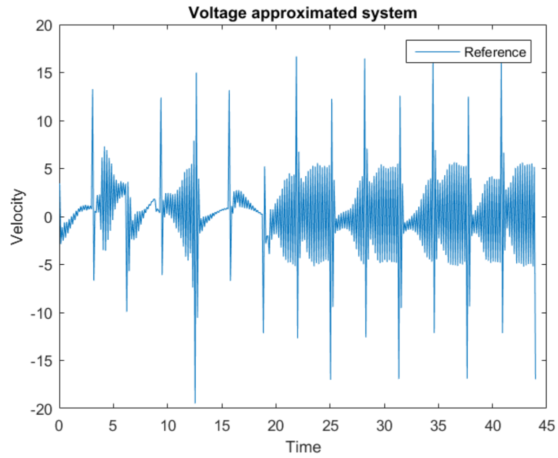


(b) Voltage response

Figure 10: Response from position controller

This system has a rise time of 0.33 s, overshoot of 0.08 (2%) and a minimal steady state error, though it occasionally, but not always, has some oscillations.

## Level 2

The controller used in level 1 is designed directly in the discrete plane. To compare admissable sampling times, a continuous time controller is designed and then discretized with Tustins approximation.

The design steps are the same as the output feedback design in the velocity controller case and are therefore not stated again. For the feedback controller, a continuous PID with low pass filter is chosen,

$$\frac{S}{R} = \frac{s_2 s^2 + s_1 s + s_0}{s(s+_0)}. \tag{24}$$

The Diophantine equation yields the parameter values

$$r_0 = 2\omega_3\zeta - b + \omega_1 + \omega_2, \tag{25}$$

$$s_0 = \frac{\omega_1\omega_2\omega_3^2}{a}, \tag{26}$$

$$s_1 = \frac{\omega_3(2\omega_1\omega_2\zeta + \omega_1\omega_3 + \omega_2\omega_3)}{a}, \tag{27}$$

and

$$s_2 = \frac{1}{a}(-2b\omega_3\zeta + 2\omega_1\omega_3\zeta + 2\omega_2\omega_3\zeta + b^2 - b\omega_2\omega_1\omega_2\omega_3^2), \tag{28}$$

where

$$A_m A_o = (s + \omega_1)(s + \omega_2)(s^2 + 2\omega_3\zeta s + \omega_3^2). \tag{29}$$

The feedback polynomial becomes

$$\frac{T}{R} = \frac{t_0(s^2 + 2\omega_3\zeta s + \omega_3^2)}{s(s + r_0)}. \tag{30}$$

Designing the controller is done by iteration and testing. Firstly, the speed and performance of the system is set by moving the $A_m$ polynomial so that a good mix of model disturbance and sensor noice rejection is found. The closed loop poles in $A_o$ are then placed to get the desired performance. The sampling rate is first set by the thumbrule that it should be 10-30 times faster than the fastest pole in the system, then it is tuned to see what the maximum reachable sampling time is while maintaining the perfomance within specifications. The controllers are approximated using the sampling time and tested on the physical plant. The resulting control law, sampling time and perfomance is displayed below.

The control law, given in the same form as in Equation (18), is

$$(z^2 - 0.895z - 0.105)u(z) = (12.1z^2 - 9.21z + 1.75)r(z) - (114z^2 - 187z + 77.7)y(z) \tag{31}$$

with the input $u(z)$, reference $r(z)$ and the output $y(z)$. The closed loop system has a double pole in -18 and the observer polynomial has a real double pole in -45. The samlpling time is 0.02 s. The step response with corresponding voltage input is given below

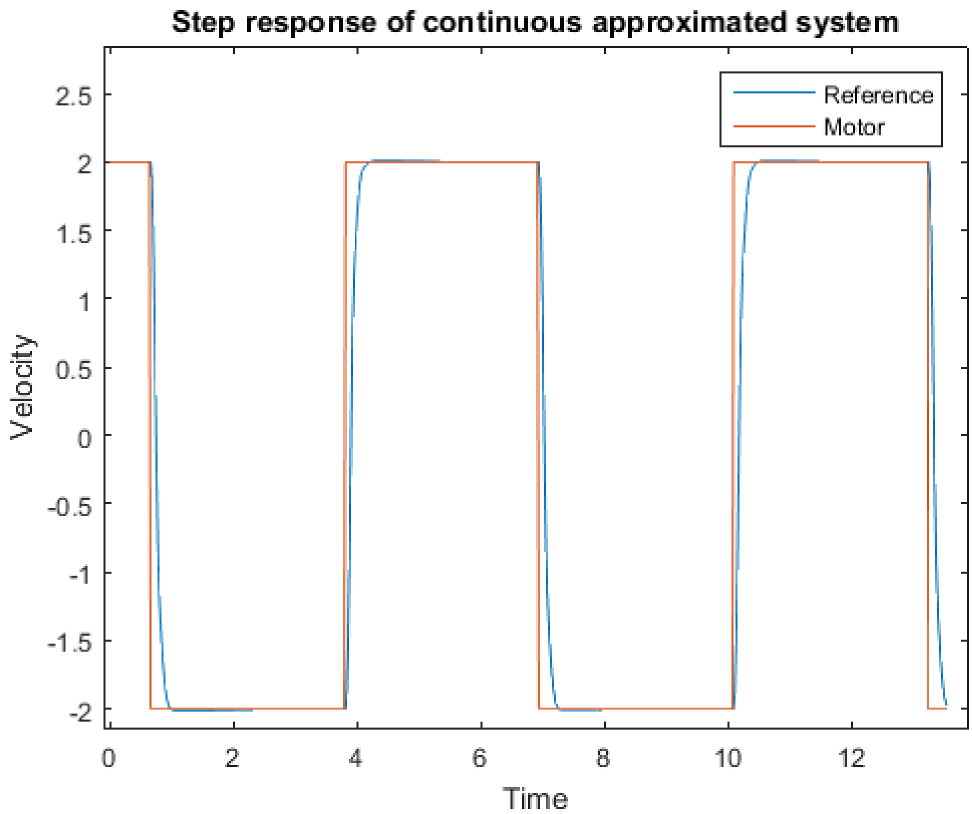


Figure 11: Step response of continuous system approximated with Tustin.

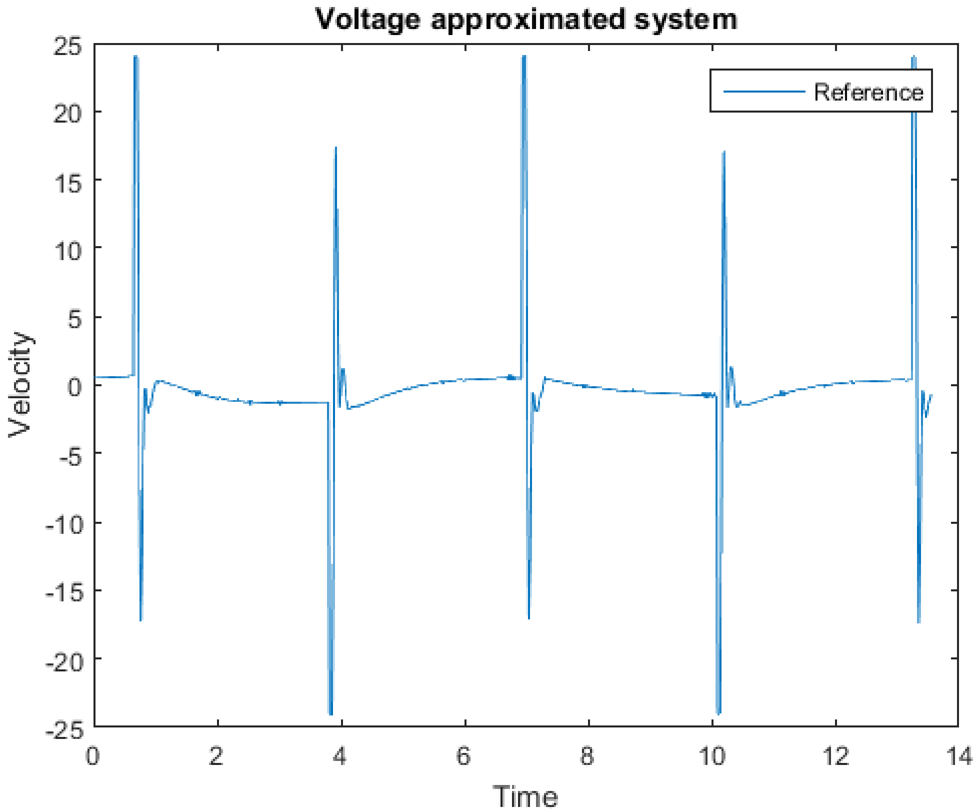


Figure 12: Voltage input of continuous system approximated with Tustin.

This system has a rise time of 0.31 s, an overshoot of 0.02 and no steady state error and as such fulfills the system requirements.

It can be seen that the sampling period can be made substantially longer when designing the system directly in the discrete plane. Since the sampling time in the continuous system is set by the fastest poles in the system, it is very dependant on the system in question. In this case, the observer polynomial was rather fast, greatly limiting the available sampling time. Furthermore, the use of approximations for the controllers may cause different mapping of poles depending in the sampling rate, putting further constraints on what sampling times are available. In this case Tustins approximation is used which always maps stable continuous poles to stable discrete poles but the Euler approximations are not guaranteed to do this.